Concealment of Damaged Block Transform Coded Images Using Projections onto Convex Sets

Huifang Sun, *Senior Member, IEEE*, and Wilson Kwok, *Member, IEEE*

Abstract— An algorithm for lost signal restoration in block-based still image and video sequence coding is presented. Problems arising from imperfect transmission of block-coded images result in lost blocks. The resulting image is flawed by the absence of square pixel regions that are notably perceived by human vision, even in real-time video sequences. Error concealment is aimed at masking the effect of missing blocks by use of temporal or spatial interpolation to create a subjectively acceptable approximation to the true error-free image. This paper presents a spatial interpolation algorithm that addresses concealment of lost image blocks using only intra-frame information. It attempts to utilize spatially correlated edge information from a large local neighborhood of surrounding pixels to restore missing blocks. The algorithm is a Gerchberg-type spatial domain/spectral domain constraint-satisfying iterative process, and may be viewed as an alternating projections onto convex sets method.

I. INTRODUCTION

IN block transform coding, the spatial redundancies within blocks are removed, and the energy is compacted into a small number of coefficients after the transformation. Compression is achieved by assigning more bits to code the high energy coefficients and less bits to the low-energy coefficients. The compressed data can be stored or be transmitted through a communication channel. Practical communication channels are not error free, although the loss mechanism may vary widely from media to media. Data corruption may be caused by network congestion, thermal noise, switch noise, signal fade, etc. Since the signals transmitted on real-world channels are highly compressed, independent of cause, the quality of images reconstructed from any corrupted data can be very unsatisfactory.

Error concealment is intended to ameliorate the impact of channel impairments (i.e., bit-errors in noisy channels or cell-loss in packet networks) by utilizing *a priori* information about typical images in conjunction with available picture redundancy to provide subjectively acceptable renditions of affected picture regions. The concealment process must be supported by an appropriate transport format that helps to identify image pixel regions that correspond to lost or damaged data [8]. Once the image regions to be concealed are identified, a combination of spatial and temporal replacement techniques may be applied to fill in lost picture elements.

In this paper, we introduce a proposed method of error concealment based on projections onto convex sets (POCS) [7]. The POCS method of image restoration attempts to satisfy *a priori* characteristics typical of most natural video images. The algorithm iterates between satisfying spatial domain and spectral domain constraints, much like Gerchberg's method [9]. We investigate the proposed algorithm by performing simulation on typical video images. The algorithm is judged on how well it performs with varying degrees of error localization (i.e. how large the damaged region is). Typical rates of algorithm convergence are determined. An objective figure of merit using peak-signal-to-noise ratio will assess the improvement gains over simpler methods of concealment. Pictorial results will demonstrate the subjective quality of the restoration.

II. BACKGROUND

A. The Source of Errors

A typical block-based video source coder, such as MPEG [10], consists of the cascade of a linear transform operation, quantization, and entropy coding. Specifically in the MPEG standard, an image is segmented into nonoverlapping blocks; then each block or prediction residual block is transformed via DCT to remove spatial correlation and subsequently the DCT coefficients are quantized and entropy coded using variable length codewords. When bit errors occur in such a highly compressed bitstream, all subsequent information becomes useless until bitstream synchronization can be reestablished. Packetization is the most common way to localize errors in a bitstream, and provides for resynchronization in the case of bit errors. Packetized bitstreams are suitable for transmission via a broadcast RF channel or packet switched network. In either scenario, bit errors that occur may lead to lost packets. In the packet network context, network congestion may cause some packets to be discarded and simply not sent to the receiver. In the broadcast RF context, damaged packets may be received with uncorrectable bit errors, and there is no way to ascertain how much of the data within the packet is usable. So for practical purposes, damaged packets are treated as lost packets.

Packets contain a known number of image data segments. For our purposes, a basic unit of image data will be taken as a 16 × 16 pixel block of image samples. A packet will contain one or more of these blocks. Loss of a packet therefore results in loss of a known quantity of blocks in the image. In the following, we first consider the restoration of a lost block surrounded by good blocks. Later, we address situations where adjacent blocks are also lost.
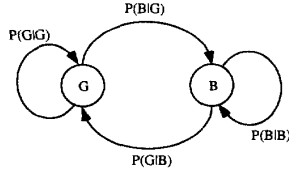
Fig. 1. Markov discrete channel model.

B. Discrete Channel Model

A discrete channel model is used because our studies involve only discrete packet quantities. The model will characterize the channel at the packet level and not at the physical waveform level. A simple channel model often employed for the simulation of bursty error sequences is a two-state Markov chain, as shown in Fig. 1. The two states correspond to reception of a (G)ood packet or a (B)ad packet. This model can describe the types of error dependence in real channels, and is suggested by experimental data [5]. Two parameters for this model have to be specified: the probability of receiving a bad packet given the previous received packet was good $(P(B \mid G))$ and the probability of receiving a bad packet given the previous packet was bad $(P(B \mid B))$. Alternatively, we may specify an average packet error probability and a mean burst length of consecutive lost packets. The average packet error probability is given by

$$P(B) = P(B \mid G)/[1 - P(B \mid B) + P(B \mid G)] \quad (1)$$

and the mean burst length is given by

$$L_B = 1/[1 - P(B \mid B)] \quad (2)$$

C. Image Degradation Model

Packet losses manifest themselves as an erasure of pixel regions in video images. An illustration in one dimension is shown in Fig. 2. Signal f is the ideal image without error, and g is the corrupted image. The degradation can be expressed as

$$g = Hf \quad (3)$$

The degradation operator H acts to admit some values of f unchanged and nulls out the others. The degradation caused by H is abrupt. H is rank deficient, and so it cannot be directly inverted to estimate f. The pseudo-inverse H^+ does not serve to give a useful estimate of f because $H^+ = H$, and so the
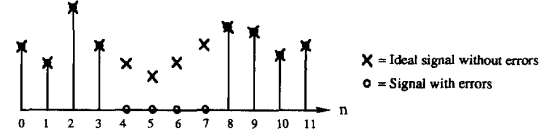

Fig. 2. Example of packet-loss degradation.

pseudo-inverse estimate $f^+ = H^+g = Hg = g$. Therefore, in order to restore a useful estimate of f, we must rely solely on a priori constraints about the class of images to which f belongs.

D. Previous Related Work

The problem of lost data in block-coded images due to imperfect communication channels needs to be solved. In particular, a good spatial interpolation method is necessary for hiding the effect of missing blocks in still images and video frames. Temporal interpolation, or replenishment, by itself is not always adequate for concealment of errors in video sequences. This is especially true for stressful image sequences with irregular motion, abrupt scene changes, and intra-coded image frames that are treated as still images. To the viewer, poor temporal replacement of error regions appear as portions of the image being broken up into displaced pieces. Earlier consideration of a spatial interpolation alternative was addressed in Wang and Zhu [1]. In that work, the spatial error concealment used an approach of interpolating a single-pixel wide boundary around the missing block to achieve a restoration based on an optimal measure of smoothness. The damaged blocks were restored fairly well in very low-frequency portions of the image. However, the smoothing process restores blurry blocks with a significant loss of detail in higher frequency portions of the image.

In this paper, we seek to utilize spatially correlated information more thoroughly by performing interpolation based on a large local neighborhood of surrounding pels and to restore edges that are continuous with those present in the neighborhood. Ramamurthi and Gersho [2] have demonstrated that edges play an important role in the subjective quality of images, and have developed a post-processing algorithm to reduce blocky artifacts caused by low bit-rate VQ. It performs nonlinear space-variant filtering that adapts to the shape of the local signal spectrum and effectively smooths out the "staircase" noise with filters aligned parallel to edges. Some of the concepts in [2] used to estimate the local edge characteristics in images, and their use of directional filters, can be applied to our application of restoring lost image blocks.

III. PROPOSED METHOD

Space variant restoration is a method of adaptively filtering a degraded image to suit the local image characteristics. To proceed with this objective, we need to estimate from the decoded image whether the missing block to be restored belongs to a monotone or edge area of the image. If the block belongs to an edge portion of the image, we must further estimate the orientation of the edge. Information obtained from the surrounding valid decoded blocks are used as an aid in
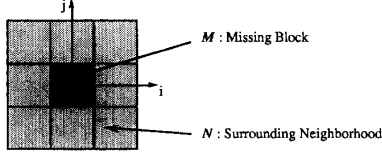
Fig. 3. Missing block of pixels with surrounding neighborhood of good pixels.
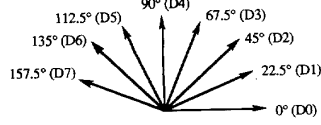

Fig. 4. Eight directional edge categories.

determining edge angle. Once the missing block area has been classified to be monotone or an edge of particular orientation, a filter specific to the class identified is then applied to restore the missing block.

A. Block Classifier and Edge Orientation Detector

Lost image blocks are restored by extending edges present in the surrounding neighborhood so that they pass through the missing block. If no edges are present in the surrounding neighborhood, the lost block is restored by a smoothing process. To accomplish this, the presence or absence of edges must be determined; if edges are present, the most likely edge orientation should be correctly chosen based on some knowledge of the edge characteristics around the missing block. A reasonably simple and effective method of performing this classification is through the use of gradient measures in the spatial domain. The local edge gradient components for the pixel $x(i, j)$ is computed by

$$g_x = x_{i+1,j-1} - x_{i-1,j-1} + 2x_{i+1,j} - 2x_{i-1,j}$$
$$+ x_{i+1,j+1} - x_{i-1,j+1} \tag{4}$$

$$g_y = x_{i-1,j+1} - x_{i-1,j-1} + 2x_{i,j+1} - 2x_{i,j-1}$$
$$+ x_{i+1,j+1} - x_{i-1,j-1}. \tag{5}$$

This is equivalent to applying the 3×3 Sobel mask operators

$$S_x = \begin{bmatrix} -1 & 0 & 1 \\ -2 & 0 & 2 \\ -1 & 0 & 1 \end{bmatrix} \qquad S_y = \begin{bmatrix} 1 & 2 & 1 \\ 0 & 0 & 0 \\ -1 & -2 & -1 \end{bmatrix}. \tag{6}$$

The magnitude and angular direction of the gradient at coordinate (i, j) are

$$G = \sqrt{g_x^2 + g_y^2} \qquad \theta = \tan^{-1}(g_y/g_x). \tag{7}$$

The Sobel operator is selected for gradient estimation due to its circularity property [6], which gives more accurate angle estimates over the standard gradient operator. Fig. 3 illustrates the missing block of pixels, denoted by M, surrounded by a neighborhood of correctly received pixels, denoted by N. The gradient measure is computed for every (i, j) coordinate in the neighborhood surrounding the missing macroblock. The value of the gradient angle is rounded to the nearest $22.5°$ and
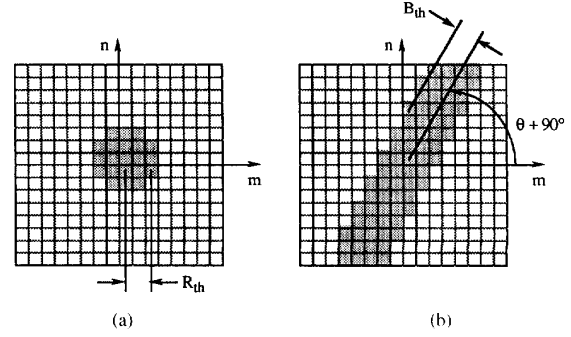

Fig. 5. (a) Lowpass filter; (b) bandpass directional filter.

thus corresponds to one of eight directional categories equally spaced around $180°$, as depicted in Fig. 4. There are counters for each of the eight directions, D_0 through D_7. A voting mechanism is used that involves incrementing the selected category counter by the magnitude of the gradient if a line drawn through the pixel at (i, j) with orientation θ passes through the missing block. This is described by the following pseudo-code

DO [over all (i, j) pixel coordinates in neighborhood N] {
 Compute G and θ from equation (7)
 $k = [\text{round}(\theta/22.5°) + 8] \mod 8$
 if [line drawn through (i, j) with angle θ
  intersects M] {
   $$D_k = D_k + G$$
  }
}. $\tag{8}$

After all the pels in the surrounding neighborhood have "voted," the counter containing the largest value determines which direction to use in the interpolation

$$k_{\text{max}} = \underset{k}{\arg\max}(D_k). \tag{9}$$

If the largest counter value is below a certain threshold value, T, then there is no discernible edge orientation and the block is classified to belong to a monotone portion of the image

if $[D_{k_{\text{max}}} < T]$ {
  $M \in MONOTONE\ AREA$
} else {
  $M \in EDGE\ AREA$ with orientation given
   by index k_{max}
}. $\tag{10}$

Now the missing block has been classified as being a monotone block or an edge block with a particular orientation.

B. Projections onto Convex Sets

An iterative technique for restoring the damaged image blocks can be developed based on the method of projections onto convex sets (POCS). POCS has been applied to various

image restoration problems where *a priori* information can be used to constrain the size of the feasible solution set [3], [4]. These constraints can be used at the receiver to implement algorithms that generate an estimate of the image to be restored. There are *a priori* properties about typical video images we would like to use; these include:

1) Smoothness—requires reconstructed samples to be smoothly connected with adjacent samples
2) Edge Continuity—requires that edges of objects in the scene be continuous
3) Consistency with known values—requires that correctly received sample values not be altered by the restoration process, and that restored values lie in a known range (e.g. [0–255]).

The goal is to formulate these desired properties as convex constraints.

Common constraints such as space-limiting, band-limiting, nonnegativity, and bounded energy are known to be convex sets [7]. To characterize the desired image properties enumerated above, we make use of the following convex constraints and projection operators:

1) *The class of signals that takes on a prescribed set of known values*: This set C_1 containing all signal vectors x in n-dimensional real space R^n with some components equal to known values can be expressed as

$$C_1 = \{x \in R^n : x_i = k_i, i \in I\} \quad (11)$$

where x_i is the ith component of vector x, and k_i are known constants in a given index set I. The projection operator P_1 onto convex set C_1 is given by

$$[P_1 x]_i = \begin{cases} k_i, & i \in I \\ x_i, & \text{otherwise.} \end{cases} \quad (12)$$

This projection operates as follows: if the value of the component is known, then this value is assigned to the projection; otherwise, it is left unchanged.

2) *The class of signals that takes on a prescribed set of transform coefficients*: This set C_2 containing all signal vectors x in n-dimensional complex space C^n with some transform coefficients equal to known values can be expressed as

$$C_2 = \{x \in C^n : [Tx]_i = z_i, i \in I\} \quad (13)$$

where T is a linear transform operator, $[Tx]_i$ is the ith transform coefficient, and z_i are known constants in a given index set I. The projection operator P_2 onto convex set C_2 is given by

$$[T P_2 x]_i = \begin{cases} z_i, & i \in I \\ [Tx]_i, & \text{otherwise.} \end{cases} \quad (14)$$

If the transform coefficient is prescribed, the projection is assigned that coefficient; otherwise, it is left unchanged.
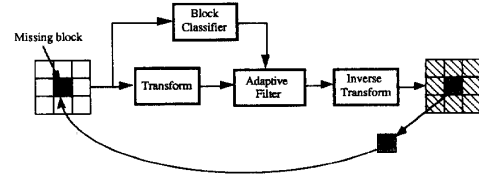

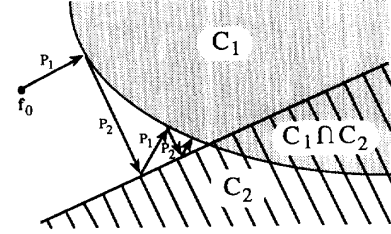Fig. 6. Adaptive POCS iterative restoration process.

Fig. 7. Signal space illustration of projections onto convex sets.

Projection operator P_1 can be used to impose the constraint of consistency with known values. Any signal vector x representing an image over this region shown in Fig. 3 can be forced to satisfy consistency with the following projection

$$[P_1 x]_{i,j} = \begin{cases} k_{i,j}, & (i,j) \in N \\ 0, & (i,j) \in M \text{ and } x_{i,j} < 0 \\ 255, & (i,j) \in M \text{ and } x_{i,j} > 255 \\ x_{i,j}, & \text{otherwise} \end{cases} \quad (15)$$

where (i,j) are the pixel indices, and $k_{i,j}$ are the correctly received neighborhood pixel values.

Projection operator P_2 can be used to impose smoothness and edge continuity constraints. P_2 is adaptive to the local image characteristics. In monotone areas of the image, the spectrum is nearly isotropic and has very low bandwidth. So, for missing blocks classified to belong to monotone areas, we can impose the constraint that any feasible restoration must have a lowpass bandlimited spectrum (i.e., must be smooth). Specifically in this case, convex set C_2 becomes

$$C_{2,SMOOTH} = \{x \in C^n : [Tx]_{m,n} = 0, \sqrt{m^2 + n^2} > R_{th}\} \quad (16)$$

where T is the 2-D $N \times N$ discrete Fourier transform operator, (m,n) specify indices to a Fourier coefficient with $-N/2 \leq m, n \leq N/2 - 1$, and R_{th} is a threshold radius that specifies the lowpass cutoff frequency. Projection operator P_2 then becomes

$$[T P_{2,SMOOTH} x]_{m,n} = \begin{cases} 0, & \sqrt{m^2 + n^2} > R_{th} \\ [Tx]_{m,n}, & \text{otherwise.} \end{cases} \quad (17)$$

So $P_{2,SMOOTH}$ acts as a lowpass filter that sets high frequency coefficients located outside the bandwidth radius specified by R_{th} to zero and leaves low-frequency coefficients unchanged. Fig. 5(a) illustrates the filter corresponding this projection. The shaded regions denote the passband of the filter with unity gain and the unshaded regions denote the stopband of the filter with zero gain. In edge areas of the image,
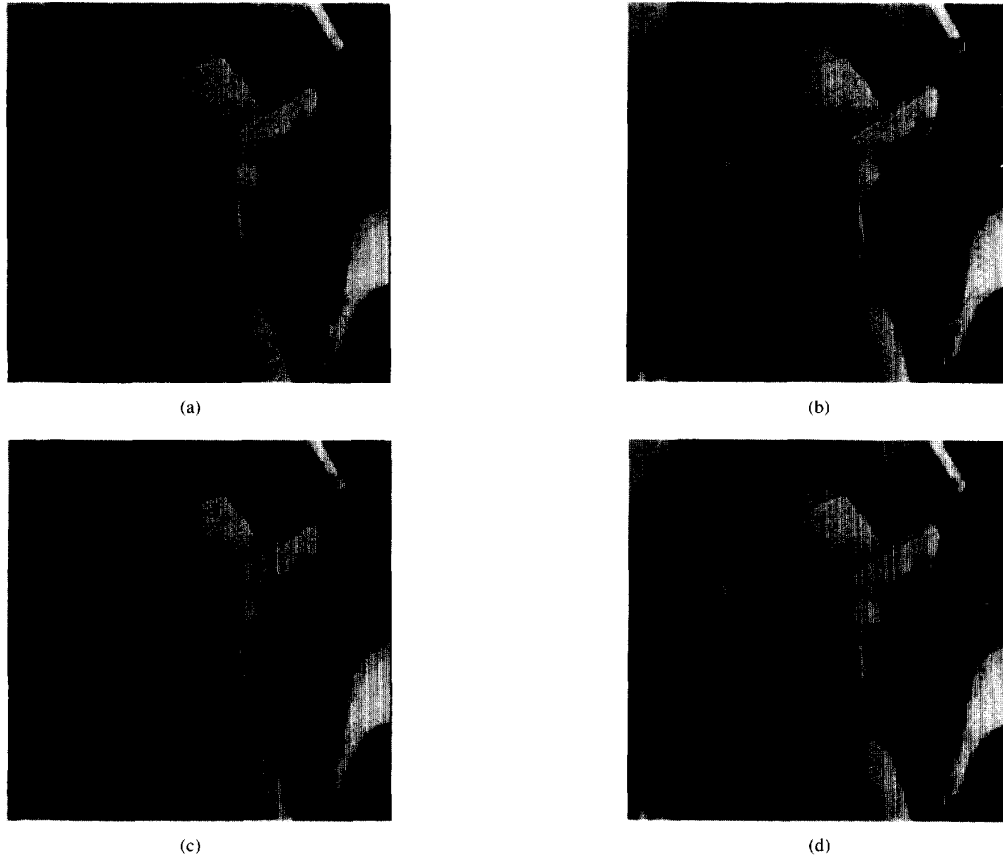
(a)

(b)

(c)

(d)

Fig. 8.   Isolated lost block experiment. (a) Original "Lena" image. 512 × 512; (b) damaged image with lost blocks concealed with neighborhood mean value (20.26 dB); (c) smooth POCS restoration (21.33 dB); (d) adaptive smooth/edge POCS restoration (23.93 dB).

the spectrum has a bandpass characteristic in which energy is localized in transform coefficients that lie in a direction orthogonal to the edge; the other remaining coefficients are very small. So for missing blocks classified to belong to edge areas, we can impose the constraint that any feasible restoration must have a bandpass spectrum oriented orthogonal to the classified edge. Specifically in this case, convex set C_2 becomes

$$C_{2,EDGE} = \{x \in C^n : [Tx]_{m,n} = 0,$$
$$|m - n * \tan(\theta + 90°)| > B_{th}\}   (18)$$

where T is the 2-D $N \times N$ discrete Fourier transform operator, (m, n) specify indices to a Fourier coefficient with $-N/2 \leq m, n \leq N/2 - 1$, θ is the angle of the classified edge, and B_{th} is a threshold bandwidth. Projection operator P_2 then becomes

$$[T P_{2,EDGE}x]_{m,n}$$
$$= \begin{cases} 0, & |m - n * \tan(\theta + 90°)| > B_{th} \\ [Tx]_{m,n}, & \text{otherwise.} \end{cases}   (19)$$

So, $P_{2,EDGE}$ acts to set frequency coefficients located outside the bandpass bandwidth specified by B_{th} to zero and leaves the other frequency coefficients unchanged. Fig. 5(b) illustrates the filter corresponding to this projection operator.

These two convex projections can be used in the proposed iterative restoration algorithm shown in Fig. 6. Here, the damaged block with surrounding good blocks is used to form a large block. The large block is classified to be monotone or one of the edge directions and at the same time undergoes a Fourier transformation. The transform coefficients are filtered by the adaptive filter according the type of the large block specified by the classifier. The filtered coefficients are used to reconstruct the image using inverse transform. The portion of the reconstructed image at the location of the damaged part of the image is sent back to the input for the next iteration.

Thus, the signal to be restored is forced to satisfy the two convex constraints by alternatively projecting onto each convex set. The signal to be restored, f, can be found through the following iteration

$$f_{i+1} = P_1 P_2 f_i   (20)$$

where we have identified the following operators P_1 and P_2 as

P_2 is the projection operator corresponding to the adaptive filter, which imposes the convex constraint that certain transform coefficients are known *a priori* to be zero.

P_1 is the projection operator corresponding to copying the restored image block back into the center of the large
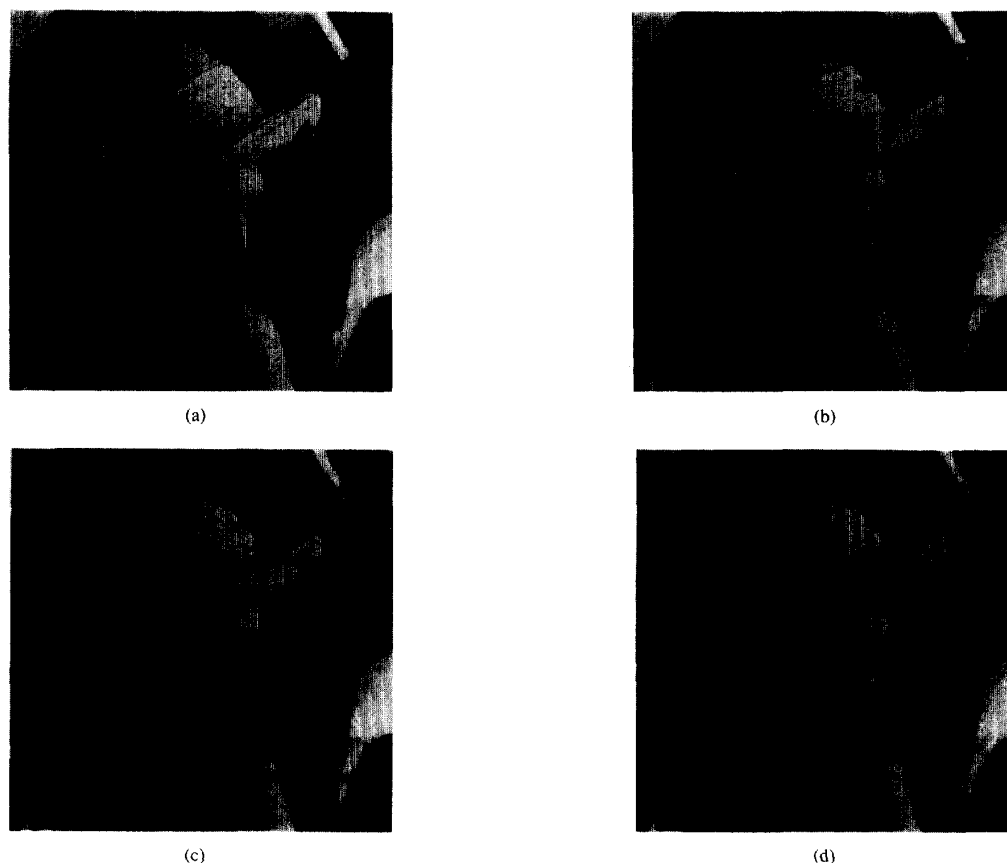
(a)

(b)

(c)

(d)

Fig. 9. Contiguous lost block experiment. (a) Original "Lena" image, 512 × 512; (b) damaged image with lost blocks concealed with neighborhood mean value (15.97 dB); (c) smooth POCS restoration (16.71 dB); (d) adaptive smooth/edge POCS restoration (18.08 dB).
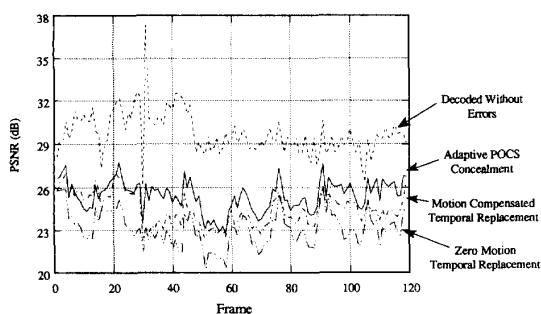

Fig. 10. Video experiment on sequence "Basketball."

Simulation Scenario	Average PSNR (dB)
Decoded Without Errors	29.74
Adaptive POCS Concealment	25.47
Motion Compensated Temporal Replacement	24.51
Zero Motion Temporal Replacement	23.18

Fig. 11. Average PSNR for the video sequence.

block, which imposes the convex constraint that forces known correctly received neighboring pixel values to remain unchanged.

If the two convex sets intersect one another, then convergence to a point of intersection is guaranteed [7]. If the two convex sets do not intersect, the algorithm will oscillate between two projection points that are in some sense "close" to both sets. Depending on where the algorithm stops, the solution will either be in one set or the other. Fig. 7 illustrates this projection process.

According to the classification, an adaptive filter is formed that either passes transform coefficients of low-frequency or transform coefficients aligned with the classified edge unchanged and zeroes out the rest. Although the adaptive filters impose constraints that are not exact *a priori* knowledge, these heuristically developed constraints form good estimates of the likely solution space. If the classified block belongs to a monotone area, we see that the algorithm acts to create a reconstructed block that is a smooth extension of neighborhood blocks. If the classified block belongs to an edge area, the algorithm acts to create a reconstructed block with an edge extended from the neighborhood pixel region. We note that this algorithm produces a restored image that is consistent with all correctly received data; good image blocks are not altered by this process.
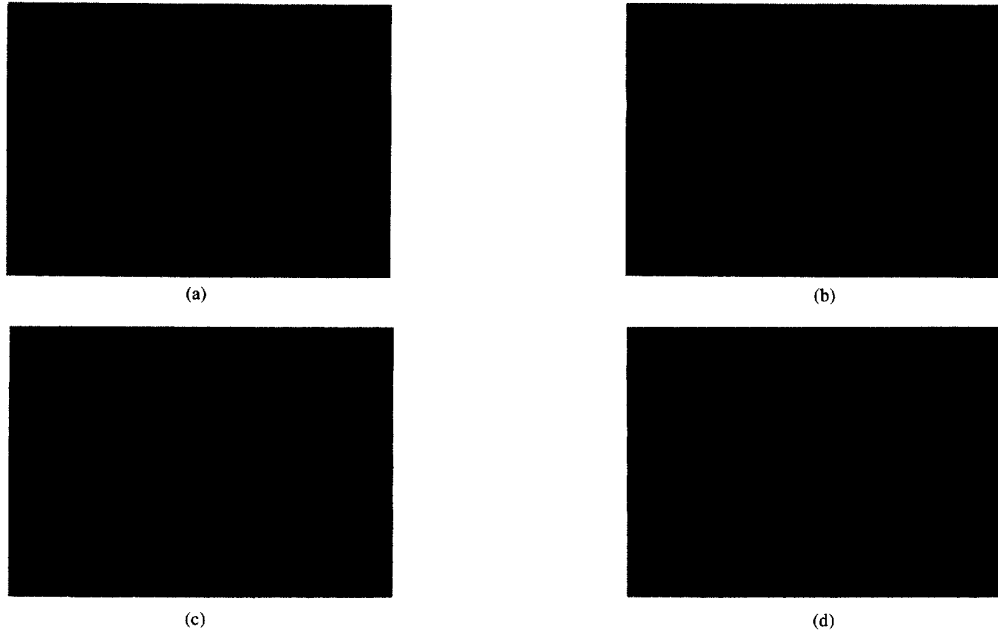
(a)

(b)

(c)

(d)

Fig. 12.   Snapshot of a P-picture from the video experiment. (a) Decoded without errors (29.46 dB); (b) zero motion temporal replacement (23.81 dB); (c) motion compensated temporal replacement (24.44 dB); (d) adaptive POCS spatial concealment (25.60 dB).

IV. SIMULATION RESULTS

The algorithm is tested on several still images and image sequences. The size of the test image is 512×512 pixels and lost blocks are 16×16 pixels. Monotone/edge gradient decision threshold $T = 5000$, lowpass filter radius $R_{th} = 3$, and bandpass width $B_{th} = 3$ were found to be suitable threshold parameters for typical images of those dimensions. Simulation results show that good restored images can be obtained after approximately five to ten iterations when the initial starting value, f_0 from (20), is set to the mean value of pixels from the neighboring blocks.

Fig. 8 shows pictorial results of a still image experiment in which lost blocks are isolated, whereby each lost block has all eight of its neighboring blocks received correctly. Fig. 8(a) is the original "Lena" picture. Fig. 8(b) shows the damaged blocks simply concealed by a constant neighborhood averaging of pixels. The blockiness present makes this simple method unacceptable in most images. Fig. 8(c) shows the results of the POCS method using only a space-invariant smoothing constraint. It is seen that blurred blocks result in the reconstructed image. Finally, Fig. 8(d) shows the results of the POCS method using adaptive classified edge constraints in addition to the smoothness constraint. The quality of the restored edges of the background vertical column, the hat rim, and Lena's lip is noteworthy. The peak signal-to-noise ratio (PSNR) serves as an objective measure of image quality, and is given by

$$PSNR = 10 \log \left(\frac{255^2}{\frac{1}{NM} \sum_{i=0}^{N-1} \sum_{j=0}^{M-1} |x(i,j) - \hat{x}(i,j)|^2} \right)$$

(21)

where $\hat{x}$ is the restored image, x is the original image, and the dimensions are $N \times M$ pixels. The PSNR's for Figs. 8(b)–(d) are 20.26, 21.33, and 23.93 dB, respectively.

Fig. 9 shows pictorial results of another still image experiment in which lost blocks occur consecutively in a row so that horizontal adjacent blocks are also lost. This scenario represents a severe case of errors when image blocks are packetized and transmitted in raster-scan order. Missing block classification is limited to an estimate based on neighboring top and bottom good blocks only. Fig. 9(a)–(d) shows the original image, mean value restoration, smooth POCS restoration, and adaptive smooth/edge POCS restoration, respectively. The PSNR's for Figs. 9(b)–(d) are 15.97, 16.71, and 18.08 dB, respectively.

The results have shown that if an edge direction is chosen correctly, the edge will be extended from the surrounding blocks to the recovered lost blocks. When strong edges are present, the classifier works well in determining which direction to use in the directional filtering. In Fig. 9(d), edges oriented close to horizontal cannot be expected to be restored as well as those oriented vertically because of the lack of valid decoded blocks on either side. Overall, the subjective quality of the image is good considering the severe damage caused by so many lost blocks.

In the video sequence simulations, quantitative results are obtained by calculating PSNR as a function of frame number. The video sequence source tested is "Basketball," which contains moderately irregular motion throughout; it consists of 720×512 pixel image frames and is encoded with an MPEG encoder at 6.0 Mbps. MPEG coding parameters [10] $M = 3$ and $N = 15$ were used, which effectively limits the extent of temporal error propagation to be less than 15

frames. The resulting bitstream is then packetized into 47-byte ATM-style data packets and errors were introduced with a cell loss probability of 10^{-2} and mean burst length of 2. In the MPEG context, a *slice* consists of an integral number of *macroblocks* grouped together in raster-scan row order. Each MPEG macroblock consists of the combination of 16 × 16 pixel luminance blocks and corresponding chrominance blocks. Upon occurrence of a lost packet, resynchronization into the bitstream begins at the start of the next slice. A slice size consisting of nine macroblocks was chosen to localize the errors. We compare the performance for four different simulation cases: 1) decoded sequence without errors; 2) decoded sequence with errors and adaptive POCS concealment; 3) decoded sequence with errors and motion compensated temporal replacement; and 4) decoded sequence with errors and zero motion temporal replacement. The zero motion temporal replacement scenario simply does a macroblock-copy of corresponding pixels from the previous reference frame, whereas the motion compensated temporal replacement scenario does a motion compensated macroblock-copy using the motion vector from the top adjacent macroblock, if available. Fig. 10 shows the results of cases 1), 2), 3), and 4) plotted on the same set of axes. Fig. 11 shows the average PSNR for all four cases. The PSNR's are computed relative to the original uncoded source images. It is observed that the adaptive POCS concealment algorithm performs better than motion compensated block-copying by 1.0 dB and better than zero motion block-copying by 2.3 dB; the adaptive POCS concealed images are within 5 dB of perfectly decoded images. In Fig. 12, a typical P-picture located in the middle of a group of pictures (GOP) is taken from the set of four simulation scenarios and displayed for comparison. These results are not intended to suggest that our spatial concealment algorithm performs better than temporal replacement in general but only in certain kinds of video sequences. When errors strike portions of video that have highly irregular motion and scene-cuts, spatial concealment will generally perform better than temporal replacement; when errors strike portions of video that have uniform, small, or no motion, temporal replacement will generally perform better. Spatial concealment can be combined with temporal replacement to obtain even better error concealment than either method alone [11].

V. CONCLUSION

Compared with the existing spatial error concealment algorithm [1], the technique proposed here has two important features. The first is the use of spatially correlated information on a large local neighborhood pels instead of a one-pixel wide boundary. In such a way, the edge information can be better estimated. Second, directional filtering is used for recovery of the missing block. In this method, a directional constraint, instead of only a smoothness constraint, is applied to the method of projections onto convex sets. The reconstruction of the lost block converges to the set with edge information specified by the directional filter. This spatial concealment technique can be used to recover the lost blocks in still images or video sequences. It can also be combined with temporal

replacement algorithms to provide improved error concealment for block-based video sequence coding.

REFERENCES

[1] Y. Wang and Q. Zhu, "Signal loss recovery in DCT-based image and video codecs," in *SPIE Proc. Visual Commun. Image Processing '91*, Boston, MA, Nov. 11–13, 1991, pp. 667–678.

[2] B. Ramamurthi and A. Gersho, "Nonlinear space-variant postprocessing of block coded images," *IEEE Trans. Acoust., Speech, Signal Processing*, vol. ASSP-34, no. 5, pp. 1258–1267, Oct. 1986.

[3] M. I. Sezan and H. Stark, "Tomographic image reconstruction from incomplete view data by convex projections and direct Fourier inversion," *IEEE Trans. Med. Imag.*, vol. MI-3, pp. 91–98, June 1984.

[4] M. I. Sezan and M. Tekalp, "Adaptive image restoration with artifact suppression using the theory of convex projections," *IEEE Trans. Acoust., Speech, Signal Processing*, vol. 38, no. 1, pp. 181–185, Jan. 1990.

[5] M. C. Jeruchim et al., *Simulation of Communication Systems*. New York: Plenum, 1992.

[6] E. R. Davies, *Machine Vision*. New York: Academic, 1990.

[7] D. C. Youla and H. Webb, "Image restoration by the method of convex projections: Part I—Theory," *IEEE Trans. Med. Imag.*, vol. MI-1, pp. 81–94, Oct. 1982.

[8] D. Raychaudhuri, H. Sun, and R. S. Girons, "ATM transport and cell-loss concealment techniques for MPEG video," in *Proc. ICASSP '93*, pp. 117–120, vol. 1.

[9] R. W. Gerchberg, "Super-resolution through error energy reduction," *Opt. Acta*, vol. 21, pp. 709–720, 1974.

[10] Moving Pictures Experts Group, "Coding of moving pictures and associated audio for digital storage media at up to about 1.5 Mbps, Part 2: Video," *ISO-IEC/JTC1 SC29/WG11*, Nov. 23, 1991.

[11] H. Sun and J. Zdepski, "Adaptive error concealment algorithm for MPEG compressed video," in *Proc. SPIE Visual Commun. Signal Processing '92*, pp. 814–824, vol. 2.

Huifang Sun (S'86–M'86–SM'93) received the B.S. degree in electrical engineering from Harbin Engineering Institute, Harbin, China, in 1967 and the Ph.D. degree in electrical engineering from University of Ottawa, Ottawa, Canada, in 1986.

Beginning in 1970, he was an engineer at the Shanghai Aeronautical Radio and Electronic Research Institute, Shanghai, China. In 1981, he was a visiting scholar at Laval University, Quebec, Canada. From 1982 to 1986, he was with the digital image processing laboratory in electrical engineering at University of Ottawa, where he served as a Teaching Assistant, Research Assistant, and post-doctoral Fellow. In 1986, he jointed Fairleigh Dickinson University, Teaneck, NJ, as an assistant professor and later as an associate professor in electrical engineering. Since 1990, he has been with the David Sarnoff Research Center (formerly RCA Laboratories), Princeton, NJ, as a Member of the Technical Staff. His current interests include digital image processing, video data compression and error concealment, visual communications, and HDTV design.
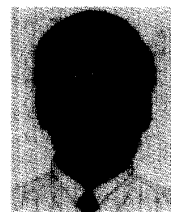
Wilson Kwok (M'93) was born in Brooklyn, NY, in 1970. He received the B.S. and M.S. degrees in electrical engineering, summa cum laude, from The Cooper Union, New York, NY, in 1991 and 1992, respectively.

In 1992, he joined the David Sarnoff Research Center, where he is now a Member of the Technical Staff. He currently works on MPEG/HDTV development. His research interests include imaging systems, image/video processing, and communication network systems.

Mr. Kwok was the recipient of the IEEE Region I student paper award in 1991 for his work on synthetic aperture radar imaging systems.